Pressure-induced phase transition in $LaAlO_3$

2002 J. Phys.: Condens. Matter 14 3981

(http://iopscience.iop.org/0953-8984/14/15/312)

INSTITUTE OF PHYSICS PUBLISHING JOURNAL OF PHYSICS: CONDENSED MATTER

J. Phys.: Condens. Matter **14** (2002) 3981–3991 PII: S0953-8984(02)33431-3

Pressure-induced phase transition in $LaAlO_3$

P Bouvier[1] **and J Kreisel**[2,3]

[1] European Synchrotron Radiation Facility (ESRF), BP 220, 38043 Grenoble Cedex, France
[2] Laboratoire des Matériaux et du Génie Physique, ENS de Physique de Grenoble, BP 46, 38402 St Martin d'Hères Cedex, France

E-mail: kreisel@inpg.fr

Received 5 February 2002, in final form 14 March 2002
Published 4 April 2002
Online at stacks.iop.org/JPhysCM/14/3981

Abstract

We report on a study of pressure-dependent structural properties of $LaAlO_3$, which is considered to be a model material of the class of 'tilted' perovskites. Our high-pressure investigation by means of Raman spectroscopy and synchrotron radiation shows that $LaAlO_3$ presents structural instabilities under pressure and undergoes a soft-mode-driven rhombohedral-to-cubic phase transition in the vicinity of 14 GPa, which can be analysed in the framework of a Landau model. The structural changes are described in terms of a collective restoring of the initially tilted AlO_6 octahedra towards the ideal cubic perovskite structure without tilting. Up to 40 GPa, the pressure dependence of the volume of the pseudo-cubic phase is described by a third-order Birch–Murnaghan equation of state with parameters $V_0 = 54.57(4)$ Å^3, $K_T = 190(5)$ GPa and $K' = 7.2(4)$.

1. Introduction

In the past, investigations of temperature- and pressure-induced phase transitions have been a rich source of information that helps in the understanding of physical and structural properties of solids, with ABO_3 perovskites being one of the largest classes investigated. In fact, perovskites form a particularly interesting class of materials because even slight modifications of the crystal structure can lead to drastic changes in physical properties, especially when there is chemical substitution or when the external conditions, such as temperature or pressure, are altered.

The ideal cubic structure of the perovskite-type oxides ABO_3 is essentially simple, with corner-linked anion octahedra BO_6, the B cations at the centres of the octahedra and the A cations in the spaces (coordination 12) between the octahedra. With respect to this ideal perovskite, structural modifications can be approximated by separating two features [1,2], namely:

(i) a rotation (tilt) of the BO_6 octahedra; and
(ii) A- or/and B-cation displacements.

[3] Author to whom any correspondence should be addressed.

In principle, depending on the actual perovskite, one or any combination of the these two features can accompany structural phase transitions. Due to the complexity of the phase transitions, the natural approach when trying to achieve a fundamental understanding of them is through the investigation of perovskites, where the phase transition is driven by only one feature. Probably the best known example is the temperature-dependent cubic-to-rhombohedral phase transition in $SrTiO_3$, which can be described as a tilting of its TiO_6 octahedra [3, 4], i.e. the phase transition involves small rotations of essentially rigid octahedra, the rotation angle being the order parameter in a Landau-theory formalism.

The phase transitions and lattice dynamics of perovskites as a function of temperature and chemical substitution are fairly well known; the aim of the present study is to extend our current understanding of perovskites with special regard to pressure-induced phase transitions. Unfortunately, modifications of the perovskite structure are often hardly apparent and are difficult to analyse by means of conventional x-ray diffraction experiments, especially in the case of oxygen-related phenomena. However, recent investigations of similar oxides under pressure using monochromatic synchrotron radiation have proved to be useful—for instance, work on $LaMnO_3$ [5], $RFeO_3$ [6] or Fe_2O_3 [7]. Raman spectroscopy is known to be an appropriate technique for the study of subtle structural modifications and has been, for instance, successfully used in the study of pressure-induced phase transitions in $BaTiO_3$ [8,9], $PbTiO_3$ [10, 11], $Na_{0.5}Bi_{0.5}TiO_3$ [12] and $KNbO_3$ [13].

$LaAlO_3$ is interesting to study for several reasons. First, at ambient conditions the rhombohedral deviation from the ideal perovskite can be approximated by a simple tilt of the AlO_6 octahedra. As a consequence, for $LaAlO_3$ one might well expect to be able to describe the eventual phase transition in a quantitative way—in contrast to the existing qualitative description of the pressure-induced phonon softening in $ATiO_3$ (A = Ba, Pb, $Na_{0.5}Bi_{0.5}$) [8–12], which is driven by tilting *and* cation displacement. Further interest in $LaAlO_3$ stems from the fact that it is widely used as a substrate for thin-film growth of perovskite structures or structures containing perovskite-type structural blocks like high-temperature superconductors [14, 15]. It is well known that the deposition of thin films can lead to large strain effects at the film–substrate interface and, therefore, it is of interest to get a better understanding of the effect of pressure on $LaAlO_3$. Here we present a high-pressure investigation of $LaAlO_3$ by Raman spectroscopy complemented with synchrotron x-ray diffraction. To the best of our knowledge, there are no reports on the pressure-dependent behaviour of $LaAlO_3$ in the literature.

2. Experimental details

The $LaAlO_3$ powder investigated ($a = 5.36$ Å, $c = 13, 11$ Å at ambient conditions) was a commercially available product (CrysTec, D). Raman spectra were recorded in back-scattering geometry with a Dilor XY multichannel spectrometer equipped with a 20 times microscope objective. The 514.5 nm line of an Ar^+-ion laser was used as the excitation line. High-pressure experiments were performed in a diamond anvil cell (DAC) with diamond tips of diameter 400 μm, using a 16:4:1 methanol–ethanol–water mixture as a pressure-transmitting medium. The powder was placed in a chamber 250 μm in diameter and 50 μm thick and the pressure was monitored via the shift of the $^2F_g \Rightarrow {}^4A_{2g}$ fluorescence bands of Cr^{3+} ions in a small ruby crystal placed in the vicinity of the sample [16]. $LaAlO_3$ was studied from ambient pressure up to 15 GPa. The Raman spectra were decomposed into individual Lorentzian components using the Jandel PEAKFIT software.

Complementary high-pressure synchrotron x-ray diffraction experiments were performed at the European Synchrotron Radiation Facility (ESRF) on the ID30 high-pressure beamline. The sample was loaded in a DAC with diamond tips of diameter 350 μm. Nitrogen was used

as the pressure-transmitting medium, which implies a filling of the high-pressure cell at low temperature where nitrogen is in a liquid state. As a matter of fact, nitrogen has the advantage of being a very good transmitting medium since its low compressibility allows working under hydrostatic conditions even at high pressures, in contrast to other mediums that (partially) crystallize under high pressure. Just as for the Raman experiments, the pressure was measured using the ruby fluorescence method [16]. X-ray diffraction patterns were collected in an angle-resolved geometry on an image plate detector (Mar345) with a focused monochromatic beam at wavelength $\lambda = 0.3738$ Å. The sample-to-detector distance and the image plate inclination angles were precisely calibrated using a silicon standard. After removal of spurious peaks (coming from the diamond cell), the two-dimensional diffraction images were analysed using the ESRF Fit2D software [17], yielding intensity versus 2θ diffraction patterns. The data were analysed by profile matching (Le Bail) and by full Rietveld refinements using Fullprof software [18]. The refined parameters are the scale factor, Chebyshev polynomial background, lattice parameters (a, c), fractional coordinates of oxygen atoms and isotropic thermal parameters. The peak shapes were described with a pseudo-Voigt function. The profile parameters u, v, w, lx, ly were obtained from the refinement of a high-purity silicon standard.

3. General considerations

At ambient conditions $LaAlO_3$ crystallizes in a rhombohedral structure with space group $R\bar{3}c$ (D^6_{3d}). The ten atoms in the unit cell of rhombohedral $LaAlO_3$ give rise to 27 ($\boldsymbol{k} = 0$) optical modes that can be characterized according to the space group using group theoretical methods. Such a treatment [19] leads to five Raman-active modes: $\Gamma_{Raman} = A_{1g} + 4E_g$. A vibrational pattern for these phonons has been proposed by Abrashev *et al* [19].

When the temperature is increased, $LaAlO_3$ is known to adopt the ideal cubic perovskite structure with space group $Pm\bar{3}m$ (O_h) where none of the vibrational modes is Raman active. With respect to the cubic $Pm\bar{3}m$ structure the rhombohedral structure is obtained by rotation of the adjacent AlO_6 octahedra which are tilted about the $[111]_p$ pseudo-cubic diagonal, leading to the $a^-a^-a^-$ tilt system in Glazer's notation [1]. In fact, the tilts of the AlO_6 octahedra result in doubling of the cubic unit cell and, therefore, the zone centre phonons in the $R\bar{3}c$ structure come from modes located at the Γ (0, 0, 0) and R (1/2, 1/2, 1/2) points of the cubic Brillouin zone. The general consensus is that the temperature-dependent rhombohedral-to-cubic phase transition can be described by means of a soft phonon at the Brillouin zone boundary where the order parameter can be represented by the rotation angle of the tilted octahedra. As a matter of fact, Scott [3, 20] has reported softening of the A_{1g} and the lowest E_g mode on approaching the phase transition at 800 K, where the $A_{1g} + E_g$ modes are expected to collapse towards the triply degenerate F_{2u} mode of the cubic phase.

4. Raman spectroscopy

4.1. Results

In agreement with early work by Scott [3, 20] and a more recent investigation by Abrashev *et al* [19] the Raman spectrum of $LaAlO_3$ at ambient conditions is characterized by three dominant modes: an A_{1g} mode around 125 cm^{-1} and two E_{1g} modes at roughly 155 and 465 cm^{-1}. By means of lattice dynamical calculations these three bands are assigned [19] to the tilt of the AlO_6 octahedra around the hexagonal $[001]_h$ axis, to pure vibration of the La cation in the hexagonal $(001)_h$ plane and to pure oxygen bending, respectively. Our experimental set-up does not allow observation of the low-frequency E_{1g} mode at 34 cm^{-1} (tilt of the AlO_6 octahedra around an axis perpendicular to the hexagonal $[001]_h$ axis [19]).

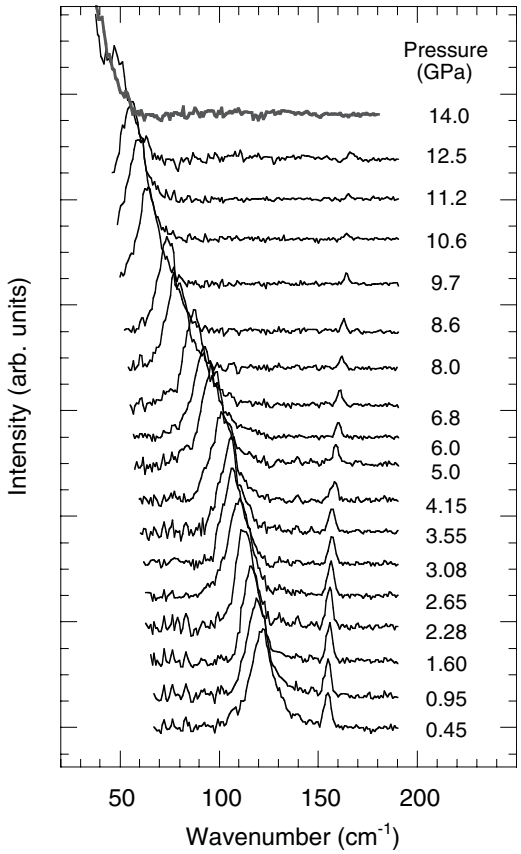

Figure 1. Pressure-dependent Raman spectra for $LaAlO_3$. The softening of the low-frequency mode accompanies a pressure-induced structural phase transition (see the text).

Figure 1 presents the pressure-dependent evolution of Raman bands initially at 124 and 154 cm^{-1} for pressures between 0.45 and 14 GPa. For pressures higher than 12.5 GPa (we performed measurements up to 15 GPa) the low-frequency A_{1g} mode was unobservable due to central Rayleigh scattering and no Raman signal was detected for the other (weaker) bands at higher frequency.

The most eye-catching spectral signature with increasing pressure is the softening of the low-frequency mode, initially at 124 cm^{-1}. Recalling that this band is related to octahedra tilts, the latter observation points to a structural phase transition involving rotations of the AlO_6 octahedra, as will be discussed in more detail in the following section. Furthermore, we observe a linear shift of the E_{1g} hard modes, initially at 154 and 488 cm^{-1}, towards higher frequencies at a rate of 0.99(2) and 1.81(5) cm^{-1} GPa^{-1} between 0.45 and 12.5 GPa, respectively (figure 2). Such linear changes under applied pressure make them useful for estimation of the pressure/strain state in $LaAlO_3$ samples.

4.2. Soft-mode frequency—phase transition mechanism

Let us now turn to the analysis of the A_{1g} band at 125 cm^{-1}; its above-addressed pressure dependence points to a pressure-induced structural phase transition involving changes in the

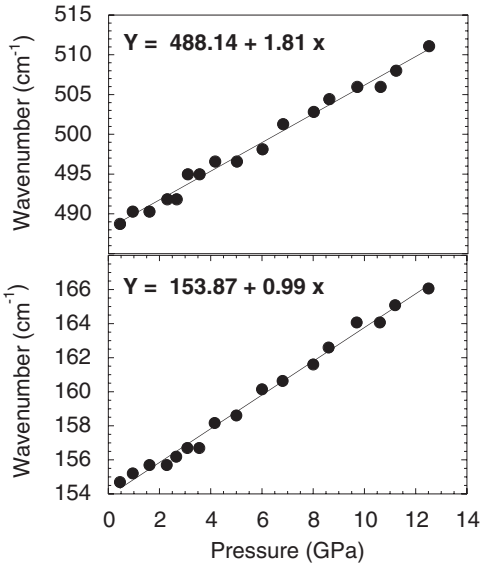

Figure 2. Band position change as a function of pressure for the modes initially at 488 and 154 cm^{-1}. The solid lines and equations are relative to a linear fit of the experimental data.

octahedron tilt. In fact, such a softening, but as a function of temperature, is observed in the Raman spectra of similar tilted perovskites, where it is often used to determine the transition temperature [3, 4, 20]. From a phenomenological point of view, the behaviour of a system in the vicinity of a symmetry-breaking structural phase transition can be described in the framework of Landau theory [21] which was in the past successfully applied in the temperature-dependent analysis of various perovskite-type materials [3]. For $LaAlO_3$ the temperature-induced structural rhombohedral-to-cubic ($R3c$-to-$Pm3m$) phase transition can be described within the Landau formalism, introducing the same multicomponent order parameters (η_1, η_2, η_3) as in $SrTiO_3$ [3], where the η_i represent out-of-phase displacements of the neighbouring octahedra (i.e. octahedra tilting). The Landau free energy (or potential) is expressed as follows:

$$\begin{aligned} F = {} & \tfrac{1}{2}A(T,P)\eta^2 + \tfrac{1}{4}B\eta^4 + \gamma_1\eta^2(e_1+e_2+e_3) + \gamma_2[3(\eta_1^2-\eta_2^2)(e_1-e_2) \\ & + (2\eta_3^2-\eta_1^2-\eta_2^2)(2e_3-e_1-e_2)] + \gamma_3(\eta_2\eta_3e_4+\eta_1\eta_3e_5+\eta_1\eta_2e_6) \\ & + \tfrac{1}{2}C_{11}(e_1^2+e_2^2+e_3^2) + C_{12}(e_1e_2+e_1e_3+e_2e_3) + \tfrac{1}{2}C_{44}(e_4^2+e_5^2+e_6^2), \end{aligned} \tag{1}$$

where $\eta^2 = \eta_1^2+\eta_2^2+\eta_3^2$ is the primary order parameter, e_i is the spontaneous strain (in the Voigt notation), C_{ii} are the appropriate elastic constants and γ_i are the coupling constants for the primary order parameter and the spontaneous strains.

The rhombohedral symmetry of $LaAlO_3$ is known to be induced by a simultaneous condensation of all three components of the order parameter (with equal magnitude $\eta_1 = \eta_2 = \eta_3$) [3]. Thus, the excess free energy reduces and the spontaneous displacement η_s is expressed in the low-symmetry phase by the standard expression

$$\eta_s^2 = -\frac{A(T,P)}{B^*} \qquad \text{with } B^* = B - \frac{6\gamma_1^2}{C_{11}+2C_{12}} - \frac{6\gamma_3^2}{C_{44}} \text{ and } A(T,P) \leqslant 0, \tag{2}$$

where B, γ_1 and γ_3 are considered as constants for varying pressure and $B^* > 0$.

In the Landau formalism, $A(T, P)$ is assumed to vary linearly with temperature. Assuming that $A(P)_T = A_0(P - P_c)$ for $P < P_c$ at fixed T, the spontaneous displacement is expected to vary as the square root of the pressure, $\eta_s(P)_T = \eta_0(P_c - P)^{1/2}$ with $\eta_0 = (A_0/B^*)^{1/2} > 0$.

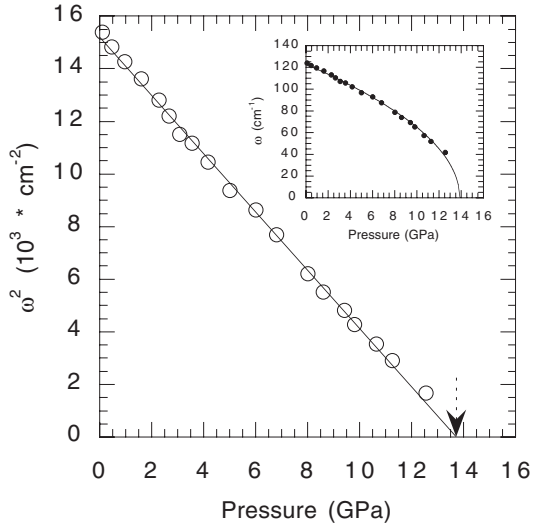

Figure 3. Pressure-dependent evolution of the squared wavenumber for the soft low-frequency A_{1g} band. The inset displays the direct band position change as a function of pressure. The solid curves are relative to least-squares fits according to equation (3) with $\omega_0 = 123.3(5)$ cm^{-1} and $P_c = 13, 75(5)$; the numbers in brackets indicate the error in the last significant figure of the fit.

The pressure dependence of the phonon frequency ω that is associated with η_s can be described in the harmonic oscillator formalism [22]:

$$m\omega^2 = \left.\frac{\partial^2 F}{\partial \eta^2}\right|_{\eta=\eta_s} = A(T, P) + 3B^*\eta_s^2 = -2A(T, P). \tag{3}$$

This leads to the following prediction for a soft mode in the low-symmetry phase:

$$\omega^2 = \omega_0^2(P_c - P) \qquad \text{for } P < P_c. \tag{4}$$

In figure 3 we have plotted the pressure-dependent data for the low-frequency A_{1g} band; there is straight-line behaviour of ω^2 versus pressure, thus validating the use of a Landau model to describe the observed structural transition. Recalling now that the order parameter (variable characterizing the symmetry change) is the angle of the AlO_6 octahedron rotation, it becomes clear that the band softening of a phonon at the Brillouin zone boundary causes a pressure-induced reduction of the rhombohedral distortion in $LaAlO_3$. The pressure-induced changes then finally lead, at around 14 GPa, to a new high-pressure phase owing to the ideal cubic structure without tilts (the $a^0a^0a^0$ tilt system, also attested to by the disappearance of the Raman spectrum). In particular, analysis of the Raman spectra does not allow access to spontaneous strain parameters. However, these can be determined by diffraction techniques.

5. Synchrotron x-ray diffraction

5.1. Structural investigation

In order to complement the above results, we have performed a high-pressure synchrotron x-ray diffraction experiment. Powder diffraction patterns were collected at a number of pressures between atmospheric and 40 GPa, using small pressure increments. Figure 4 displays a diffraction pattern obtained at low pressure together with the results from a Rietveld refinement.

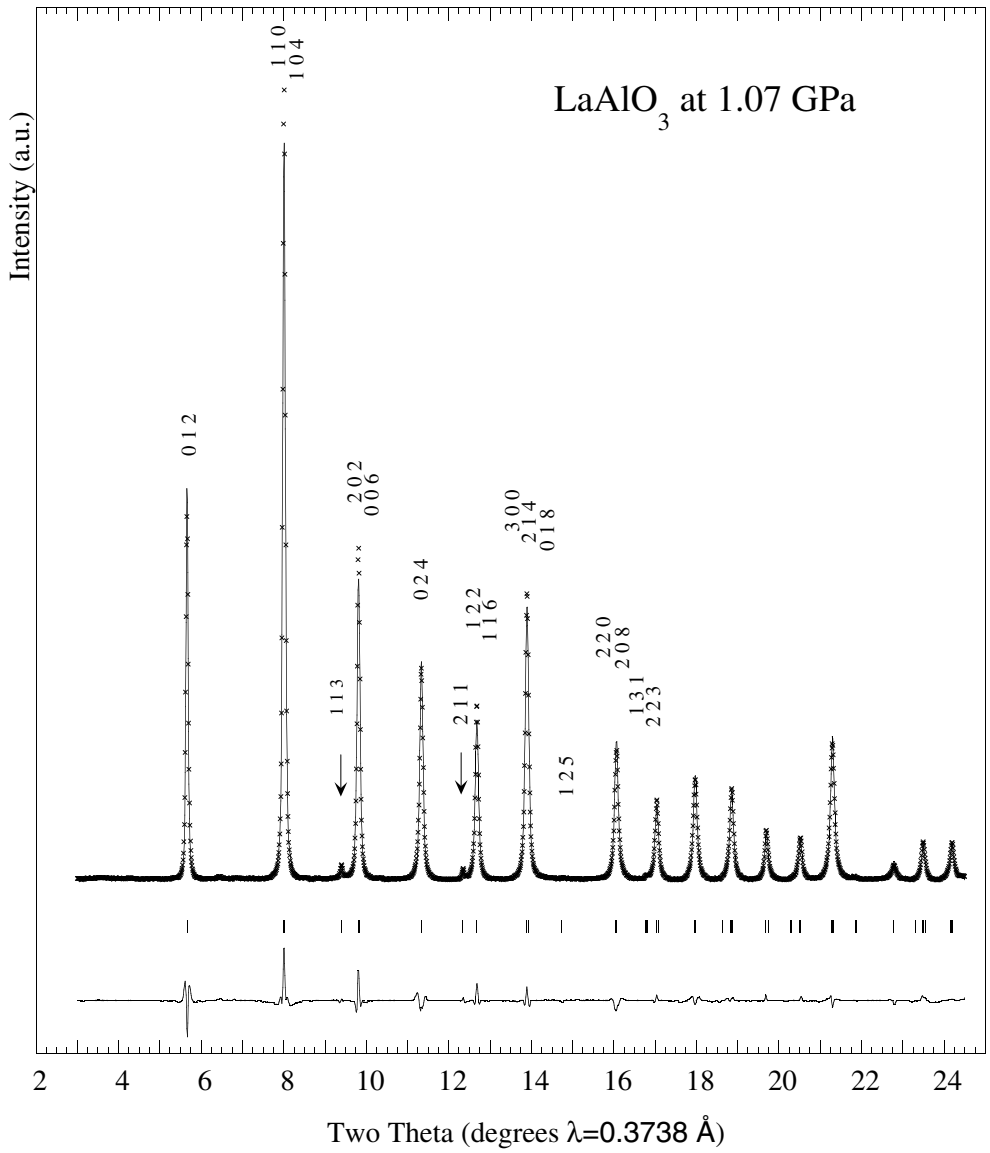

Figure 4. Results of full Rietveld refinements of the x-ray diffraction patterns of $LaAlO_3$ collected at 1.07 GPa and room temperature. The refinement leads to a rhombohedral $R\bar{3}c$ structure with La atoms on 6a sites at $(0\,0\,\frac{1}{4})$, Al atoms on 6b sites at $(0\,0\,0)$ and O cations on 18e sites at $(x\;0\;\frac{1}{4})$. The observed, calculated and difference curves are represented. The tick marks indicate the calculated Bragg reflections. Peaks indicated by arrows correspond to the superlattice reflections, which are indicative of the rhombohedral phase. The quality of the refinement is described by the conventional Rietveld R-factors, $R_p = 10.1$, $R_{wp} = 10.8$ ($R_{exp} = 9.54$), $\chi^2 = 1.28$.

There is good agreement between our results and those reported in the literature for room temperature x-ray or neutron diffraction. The $c/a\sqrt{6}$ ratio, which provides a measure of the rhombohedral distortion, is found to be equal to 0.9975(4), in good agreement with those recently reported by Howard *et al* [23]: $c/a\sqrt{6} = 0.9977(1)$. The pattern is well refined in

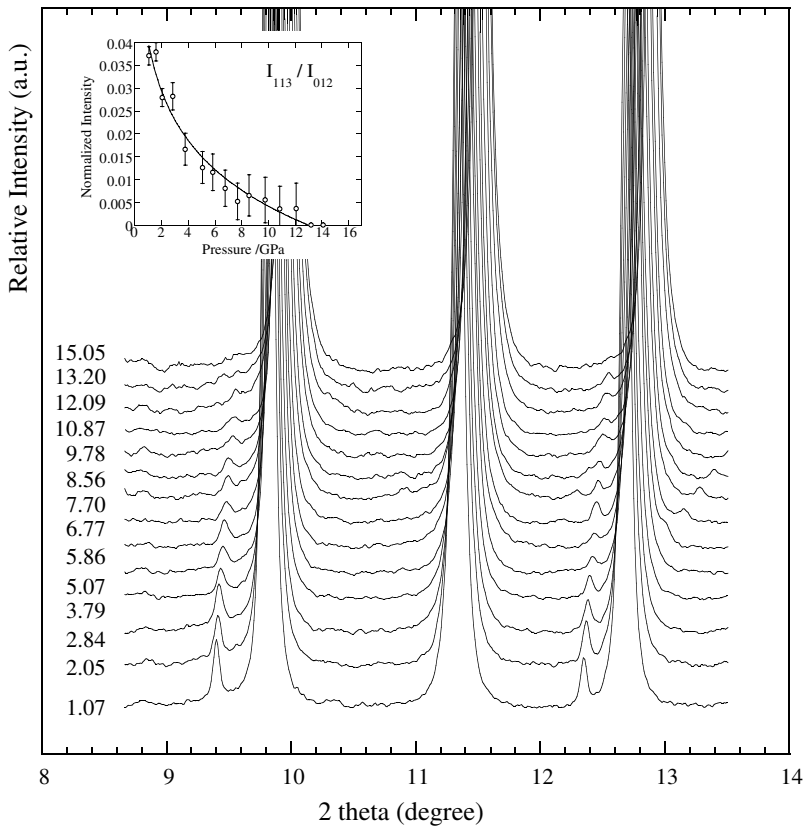

Figure 5. Pressure-dependent evolution of the enlarged x-ray diffraction pattern of $LaAlO_3$ in the 8°–14° 2θ range. The pressure is indicated on the left of each pattern. The pressure-induced phase transition towards a cubic phase is accompanied by the disappearance of the superlattice reflection for pressure higher than 15 GPa. The inset gives the pressure-dependent evolution of the intensity of the (113) superlattice reflection normalized to the (012) reflection. The later (012) reflection becomes the (100) reflection in the ideal cubic phase and is assumed not to change in intensity upon transformation.

the $R\bar{3}c$ space group with $a = b = 5.3576(13)$ Å, $c = 13.0882(16)$ Å and $x = 0.535(2)$ for the oxygen x-position.

As commonly observed for rhombohedral perovskites, it is difficult to follow in detail the pressure-dependent evolution of the rhombohedral distortion through the rhombohedral splitting of the main peaks. However, the problem of the low resolution of the rhombohedral doublet is overcome by the observation of additional weak peaks (superlattice reflections) that are associated with the $a^-a^-a^-$-type rotation of oxygen octahedra, thus giving evidence of a distortion from the cubic matrix. As shown in figure 5, the intensity of such superlattice reflections decreases gradually upon increasing pressure and, finally, for diffraction patterns above 13.2 GPa, the superlattice reflections are no longer observed. Recalling that the intensity of the superlattice reflections is determined by the x-position of the oxygen atoms (i.e. the tilt angle of the AlO_6 octahedra), the latter results are in good qualitative agreement with those from Raman scattering since they confirm both a progressive reduction of the octahedron tilt angle and a phase transition near 14 GPa. Unfortunately, the low sensitivity of the x-ray diffraction to the position of oxygen anions and the resulting weak intensity of the observed

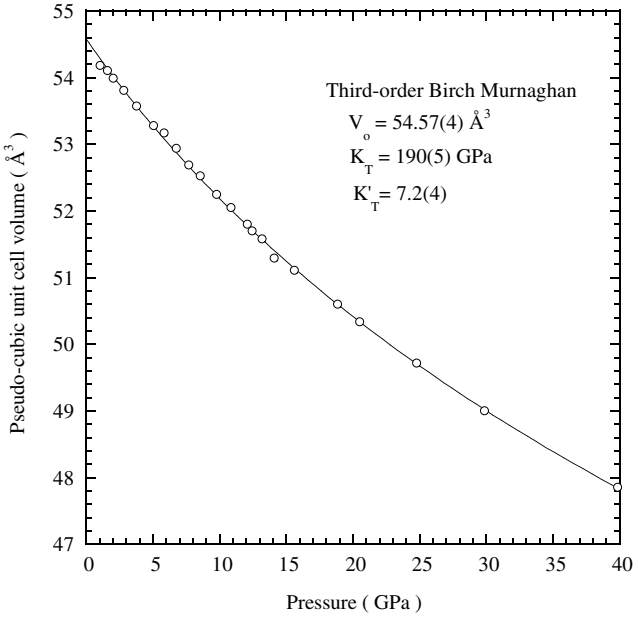

Figure 6. Pressure-dependent evolution of the unit-cell volume of $LaAlO_3$ as obtained from Le Bail refinement in the pseudo-cubic $Pm\bar{3}m$ space group. The parameters extracted from third-order Birch–Murnaghan EoS (plain curve) are equal to $V_0 = 54.57(4)$ Å^3, $K_T = 190(5)$ GPa and $K' = 7.2(4)$.

superstructure reflections (only two) in the 3°–25° 2θ range prevented a quantitative analysis of the oxygen displacement in the vicinity of the phase transition. As a consequence, the present work does not allow a full determination of the Landau potential, a point that might be addressed in the future using neutron diffraction, which is more sensitive to the position of oxygen anions.

5.2. Compressibility

In order to obtain an evaluation of the compressibility, we have performed a Le Bail refinement of the x-ray pattern in the pseudo-cubic space group $Pm\bar{3}m$ over the whole pressure range. The pressure evolution of the volume is given in figure 6. The unit-cell parameters are reported in table 1. The parameters obtained by fitting the P–V data between 1.06 and 40 GPa with a third-order Birch–Murnaghan equation of state (EoS) [24, 25] are $V_0 = 54.57(4)$ Å^3, $K_T = 190(5)$ GPa and $K' = 7.2(4)$, where V_0 is overestimated compared to the experimental value of $V_0 = 54.47$ Å^3 observed by Howard *et al* [23]. The latter is most probably due to the approximation of a pseudo-cubic space group.

6. Concluding remarks

In summary, we have investigated structural changes of $LaAlO_3$ under high hydrostatic pressure by means of Raman spectroscopy and synchrotron radiation. Our results show that $LaAlO_3$ presents pressure instabilities and undergoes, in the vicinity of 14 GPa, a soft-mode-driven rhombohedral-to-cubic phase transition, which can be described in the Landau formalism of a second-order phase transition (although the experimental data cannot provide a true proof

Table 1. Cell parameters and volumes for $LaAlO_3$ obtained from Le Bail refinements of x-ray patterns in the pseudo-cubic space group as a function of pressure. The number in brackets indicates the error in the last significant figure.

Pressure (GPa)	a (Å)	V (Å^3)
0	3.7905 [23]	54.46 [23]
1.07(1)	3.78391(16)	54.178(3)
1.60(1)	3.78208(18)	54.099(4)
2.05(1)	3.77946(18)	53.987(4)
2.84(1)	3.77513(16)	53.801(3)
3.79(1)	3.76963(15)	53.567(3)
5.07(1)	3.76273(15)	53.273(3)
5.86(1)	3.76015(14)	53.164(3)
6.77(1)	3.75472(14)	52.934(3)
7.70(1)	3.74878(17)	52.683(4)
8.56(1)	3.74496(17)	52.522(4)
9.78(1)	3.73830(18)	52.242(4)
10.87(1)	3.73362(21)	52.046(5)
12.09(1)	3.72769(17)	51.799(5)
13.20(1)	3.72228(16)	51.574(5)
14.12(1)	3.71535(10)	51.286(2)
18.85(1)	3.69805(10)	50.600(2)
20.53(1)	3.69216(11)	50.332(2)
24.80(1)	3.67701(11)	49.714(2)
29.87(1)	3.65925(11)	48.998(2)
39.87(1)	3.63055(11)	47.854(2)

of this). Recently, it has been shown that thin films might well introduce a phase change of the substrate near the interface [26]. Although our present hydrostatic pressure study does not simulate the real strain state as encountered in thin films, it gives for the first time information about intrinsic pressure-dependent structural instabilities. Here we have shown for $LaAlO_3$ that the structural instabilities with respect to pressure are relatively far from the pressures that can be met in thin films (up to 3 GPa) and thus we might plausibly expect interfacial strain not to lead to fundamental changes in the structure of $LaAlO_3$ substrates.

Acknowledgments

The authors are grateful to N Rosman for technical assistance in the high-pressure Raman study and to Professor G Lucazeau for continuous support.

References

[1] Glazer A M 1972 *Acta Crystallogr.* B **28** 3384
[2] Glazer A M 1975 *Acta Crystallogr.* A **31** 756
[3] Scott J F 1974 *Rev. Mod. Phys.* **46** 83
[4] Fleury P A, Scott J F and Worlock J M 1968 *Phys. Rev. Lett.* **21** 16
[5] Loa I *et al* 2001 *Phys. Rev. Lett.* **82** 125501
[6] Xu W M, Naaman O, Rozenberg G K, Pasternak M P and Taylor R D 2001 *Phys. Rev.* B **64** 094411
[7] Rozenberg G K, Dubrovinsky L S, Pasternak M P, Naaman O, Bihan T L and Ahuja R 2002 *Phys. Rev.* B **65** 064112
[8] Sood A K, Chandrabas N, Muthu D V S and Jayaraman A 1995 *Phys. Rev.* B **51** 8892
[9] Venkateswaran U D, Naik V M and Naik R 1998 *Phys. Rev.* B **58** 14 256
[10] Cerdeira F, Holzapfel W B and Bauerle D 1975 *Phys. Rev.* B **11** 1188

[11] Sanjurjo J A, Lopez-Cruz E and Burns G 1983 *Phys. Rev.* B **28** 7260
[12] Kreisel J, Glazer A M, Bouvier P and Lucazeau G 2001 *Phys. Rev.* B **63** 174106
[13] Gourdain D, Moya E, Chervin J C, Canny B and Pruzan P 1995 *Phys. Rev.* B **52** 3108
[14] Chakoumakos B C, Schlom D G, Urbanik M and Luine J 1998 *J. Appl. Phys.* **83** 1979
[15] Phillips J M 1996 *J. Appl. Phys.* **79** 1829
[16] Piermarini G J, Block S, Barnett J D and Forman R A 1975 *J. Appl. Phys.* **46** 2774
[17] Hammersley A 1995 *ESRF Internal Report; Fit 2D V.5 Reference Manual* EXP/AH/95-01
[18] Rodriguez-Carjeval J 1993 *Physica* B **192** 55
[19] Abrashev M V *et al* 1999 *Phys. Rev.* B **59** 4146
[20] Scott J F 1969 *Phys. Rev.* 183
[21] Landau L D and Lifshitz E M 1958 *Statistical Physics* (London: Pergamon)
[22] Slonczewski J C and Thomas H 1970 *Phys. Rev.* B **1** 3599
[23] Howard C J, Kennedy B J and Chakoumakos B C 2000 *J. Phys.: Condens. Matter* **12** 349
[24] Birch F 1974 *Phys. Rev.* **71** 809
[25] Birch F 1978 *J. Geophys. Res.* **83** 1257
[26] Vincent H, Audier M, Pignard S, Dezanneau G and Sénateur J P 2002 *J. Solid State Chem.* **164** 177